ELSEVIER

N°3

Catena 39 (2000) 187–210

CATENA

www.elsevier.com/locate/catena

Relations between soil colour and waterlogging duration in a representative hillside of the West African granito-gneissic bedrock

D. Blavet [a,*], E. Mathe [b], J.C. Leprun [a]

[a] *L.C.S.C. Institut Francais de Recherche Scientifique pour le Développement en Coopération, 911 avenue Agropolis, B.P. 5045, 34032 Montpellier, France*

[b] *Institut National des Sols, Cacavelli, Lomé, Togo*

Received 12 April 1999; received in revised form 3 November 1999; accepted 22 November 1999

Abstract

The purpose of this study was to analyse if the colour of soils on granito-gneissic bedrock of West Africa could give some simple indicators of the duration of soil waterlogging. A toposequence on a representative hillside in central Togo (lat 8°38′–8°39′N, long 1°00′–1°01′E) was studied by means of 19 hydropedological stations. Soil and piezometric conditions were studied on these stations for three annual cycles (1989–1992) during which rainfall conditions were representative of the mean rainfall conditions for that hillside. Data collected in each station were used to calculate the mean annual rate of soil waterlogging ($\overline{WLG}$) at 10-cm intervals from the surface down to a depth of 7 m. At the same intervals, 10 numerical colour variables were calculated from the colours of the uncemented soil phases: Munsell value, chroma, angular hue and redness rating of the principal uncemented phase; mean Munsell value, mean chroma, mean angular hue and mean redness rating; barycentric chroma and barycentric angular hue. Statistical relationships were established between $\overline{WLG}$ and each of the variables derived from soil colour (10 × 574 pairs). The two most significant relations were those between $\overline{WLG}$ on one hand, and mean angular hue and mean redness rating on the other. These two relationships provided the basis for logistic models for predicting the mean annual rate of soil waterlogging. The operational limits of these models are discussed.

Keywords: Soil colour; Waterlogging; Toposequence; Granito-gneissic bedrock; West Africa; Togo

* Corresponding author.
E-mail address: didier.blavet@mp1.ird.fr (D. Blavet).

0341-8162/00/$ - see front matter
PII: S0341-8162(99)00087-9

ISSN

1. Introduction

The duration of soil waterlogging by phreatic or perched groundwater is a decisive parameter for agricultural or forestry development. This parameter can vary widely over short distances, as it does on hillsides of the West African granito-gneissic bedrock (Worou, 1988; Fritsch, 1993; Blavet, 1996). However, methods previously tested on this type of hillside did not give ready access to this parameter. To monitor the water table with piezometers or tensiometers, a complex equipment array must be installed and numerous measurements taken over time (Lelong, 1966; Lenoir, 1977; Worou, 1988; Fritsch, 1993; Fritsch et al., 1990a; Blavet, 1996). Estimating the moisture status of the material by on-site measurements of ferrous iron content and oxidation–reduction potential of the soil also requires numerous measurements over time (Vizier, 1974a,b; 1984). Lastly, simulating groundwater table fluctuations from the hydrodynamic properties of the soil proves very imprecise, owing to the hydrological complexity of this type of hillside (Poss and Valentin, 1983; Chevallier, 1988). Calculating potential water saturation indices based on topography requires a very precise digital elevation model of the landform, and does not incorporate the real possibilities of water infiltration into the topsoil layers (Beven and Kirkby, 1979; Depraetere, 1992). Remote microwave sensing of groundwater location and water table level (by onboard or land-based radar) requires monitoring over time and careful calibration of the instrument; in any case its penetration depth is limited to the topsoil layers, and is considerably reduced by any clayey horizon present (Engman and Gurney, 1991; Smith et al., 1992). Finally, interpreting satellite images in the visible and infra-red parts of the spectrum requires images at different periods, and this method only allows imprecise inferences as to the location of groundwater and the level of the water table, because the vegetation that hides the soil on this type of hillside mainly depends on human activities (Poss et al., 1990).

It is therefore worth looking for simple indicators of the duration of soil waterlogging, and several arguments suggest that soil colour can be such an indicator. Theoretically, soil colour depends on the types of soil constituents present, which can depend, in turn, on the duration of soil waterlogging. It is also easily accessible and relatively stable over time. This is why several soil classification systems use soil colour in diagnosing the water regime of a soil (e.g., USDA, 1975; Vizier, 1992). Finally, several studies conducted in temperate regions have revealed significant correlations between soil colour and the duration of water saturation of the soil (Franzmeier et al., 1983; Evans and Franzmeier, 1986, 1988; Mokma and Cremeens, 1991; Mokma and Sprecher, 1994; Thompson and Bell, 1996).

Therefore, our aim was to study the relations between soil colour and the duration of soil waterlogging, on a hillside on the granito-gneissic bedrock of West Africa.

2. Materials

The study was carried out in Central Togo, in a biophysical environment covering some 500 000 km^2 in West Africa (cf. Fig. 1). This environment is characterised by a

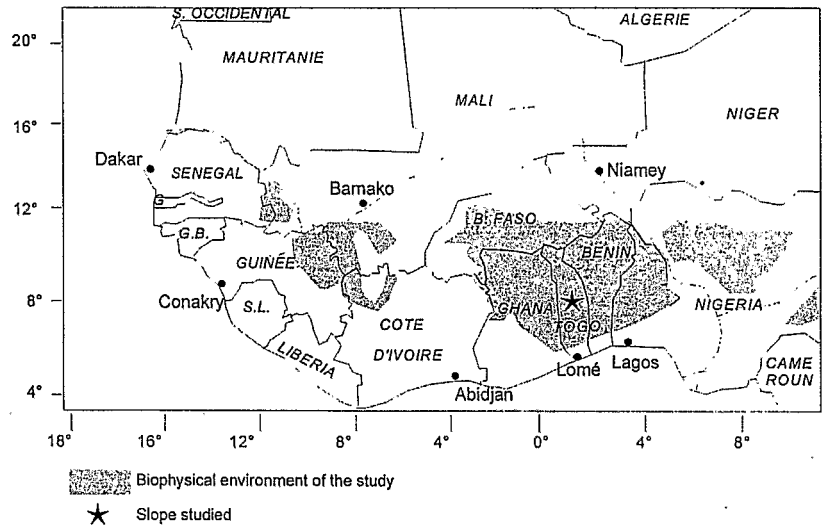

Fig. 1. Extension of the biophysical environment of this study and location of the hillside studied.

tropical climate, with a sharply contrasted dry season, a bedrock of granite and gneiss, an annual rainfall between 800 and 1200 mm, a savanna vegetation, a landform consisting of a succession of hillsides and a soil mantle which is organised in toposequences (Blavet, 1996). These toposequences consist of red ferrallitic soils upslope, derived from an ancient kaolinitic mantle (Gavaud, 1970; Boulet, 1974; Grandin, 1976; Leprun, 1979), yellow ferruginous soils at midslope positions and greenish hydromorphic soils in downslope positions (Faure, 1975; Levêque, 1975; Fritsch et al., 1990b). This sequence of soils is thought to be largely the result of transformations connected with the action of water (Chauvel, 1977; Fritsch, 1993; Blavet, 1996). The yellow horizons of the ferruginous, mid-slope soils would have formed from reddish ferrallitic soils under the effects of a temporary perched water table. Downslope, the permanent groundwater has led to bleached horizons and greenish gley in particular. A representative hillside was selected for our study. It is located on a biotite/muscovite gneiss, 300 km north of Lomé, Togo, lat 8°38′–8°39′N, long 1°00′–1°01′E (cf. Fig. 1). Mean annual rainfall is 1158 mm (1974–1992 data). There is a single rainy season centred around July–September. Mean temperature on the hillside is 25°C (1990–1992 data), with extremes of 15°C and 35°C.

On this hillside, a toposequence 650 m long was chosen, oriented along the steepest direction of slope so as to cut across all the soil mantle variants. Nineteen hydropedological stations were installed along this toposequence (cf. Fig. 2), each consisting of an array of 2–4 piezometers, observation pits, and boreholes at the piezometer sites. To reveal any perched groundwater that might be present, piezometers were placed at different depths, up to a maximum depth of 7 m, depending on drilling possibilities (Blavet, 1996). The upper part of each piezometer was coated with a bentonite sheath to seal its pores and prevent water infiltrating from above. Pierced at the lower end up to

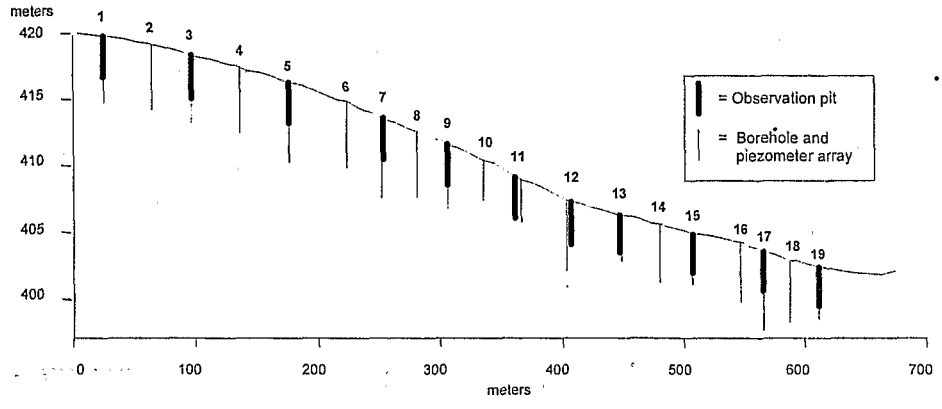

Fig. 2. Distribution of hydropedological stations along the toposequence.

30 cm from the base, these 4-cm-diameter piezometers responded to fluctuations in the water table with a negligible response time (Brand and Premchitt, 1980). The field study continued through three complete annual cycles, from September 1989 to September 1992. During this period, observation pit profiles and borehole cores were analysed, and piezometric levels were taken daily. This period was representative of rainfall conditions at the site, since mean monthly rainfall during this time differed little from the monthly median for the entire recorded pluviometric history of the site (1974–1992).

3. Methods

Taking all data at the hydropedological stations in the toposequence, statistical links were sought between soil colour parameters and duration of waterlogging. To do this,

(a) the annual soil waterlogging rate (WLG) and mean annual soil waterlogging rate ($\overline{\text{WLG}}$) were calculated at different depths;
(b) numerical parameters derived from soil colour were obtained for the same depths;
(c) correlations were sought between mean annual soil waterlogging rate and the variables derived from soil colour.

3.1. Calculation of annual and mean annual soil waterlogging rate

The mean annual soil waterlogging rate at a given point in the toposequence was defined as follows, for measurement periods of several years:

$$\overline{\text{WLG}_{xi,zi}} = 100 \times \frac{\Sigma N}{n \times 365} \tag{1}$$

with xi, zi = the spatial coordinates of the point in question (xi = position of the station in the toposequence and zi = vertical position of the measurement point), ΣN = number of days throughout the measurement period during which the water table reached the point in question, and n = number of complete years for which measurements were taken. When $n = 1$, Eq. (1) gives the annual soil waterlogging rate, which is symbolized as WLG.

This definition was used to calculate the annual and mean annual soil waterlogging rates at vertical intervals of 10 cm, for each hydropedological station in the toposequence. There were 630 measurement points in all. These calculations were made from a piezometric database of the daily readings from each array of piezometers. Annual soil waterlogging rates were calculated for each of the three annual cycles available (1989–1990, 1990–1991 and 1991–1992) and the mean annual waterlogging rate was calculated for the three cycles together (1989–1992). In practice, one piezometer was associated with each of the 630 measurement points and counted the number of days when the water table levels were equal to or above the elevation of that point. As these operations involved more than a million readings of the water table level, the calculations were made by a computer program working on the piezometric database (Blavet, 1996).

3.2. Obtaining the variables derived from soil colour

A morphological study of the profiles and core samples allowed identification of homogeneous, sub-horizontal elementary soil volumes (SVs) several centimetres to several decimetres thick. Each of these volumes was described in morphological terms (Mathé, 1993; Blavet, 1994), including their vertical boundaries and the proportion and colour of each uncemented phase. These parameters were entered in a pedological database (Blavet, 1996).

The colours of the uncemented phases were assessed by Munsell colour chart (Munsell, 1946, 1976), including Munsell hue (H_{Munsell}), Munsell value (V) and Munsell chroma (C). This operation was first carried out in the field, to identify the uncemented phases. The colour of each phase was then systematically re-assessed in the laboratory from air-dried SV samples, under constant light conditions (white-light neon tube), in order to obtain colours independent of soil moisture level and light conditions in the field.

The alphanumerical Munsell code of each colour, as re-assessed in the laboratory, was then converted into a purely numerical code. No conversion was needed for the Munsell value and Munsell chroma variables since these are numerical (the last two numbers in the code). As the Munsell hues are spread around a circle in the Munsell colour cylinder, they were converted into angular hues ($H°$), in degrees, according to their position in the circle, taking as a convention $H° = 360°$ for Munsell hue 10 RP. The formula used for this conversion was as follows:

$$H° = 36\left(I_p + \frac{I_s}{10}\right) \tag{2}$$

where I_p is the numerical coding of the Munsell hue segment concerned (i.e., Munsell hue R ⇒ 0; YR ⇒ 1, Y ⇒ 2; GY ⇒ 3; G ⇒ 4; BG ⇒ 5; B ⇒ 6. PB ⇒ 7; P ⇒ 8; RP ⇒ 9) and I_s is the number associated with that Munsell hue (i.e., 2.5 for 2.5 YR; 5 for 5 YR, etc.). This conversion gave us, for the frequently occurring soil hues, the equivalents shown in Table 1.

Redness rating (RR)(Torrent et al., 1980, 1983), which is a variable combining the V, C and H components of a colour was also taken into account. RR is linked to the mineralogical form of iron oxide present, especially its hematite content (Schwertmann, 1993). It has already been used as an indicator of soil water saturation status (Thompson and Bell, 1996). It is defined as follows:

$$\mathrm{RR} = \frac{(10 - H_r) \times C}{V} \tag{3}$$

In Eq. (3), the conventions for the hue are $H_r = 0$ for 10 R and $H_r = 10$ for 10 YR. This convention gives a grading system where the hue circle is divided into 100 units for H_r (as against 360 units for $H°$), with a displacement of one tenth of the circle (36 units of $H°$ or 10 units of H_r) between the starting point of $H°$ (10 RP) and that of H_r (10 R). Thus, the conversion between H_r and $H°$ is as follows:

$$H_r = \frac{100(H° - 36)}{360} = \frac{5H°}{18} - 10 \tag{4}$$

In this way, RR was calculated as a function of $H°$ as follows, based on Eqs. (3) and (4):

$$\mathrm{RR} = \frac{\left(10 - \left(\frac{5H°}{18} - 10\right)\right) \times C}{V} = \frac{(360 - 5H°) \times C}{18V} \tag{5}$$

In the field, the proportion of the different uncemented phases were assessed, using the field quantification scale shown in Table 2. This scale, in which the intervals are narrower at the two extremes than in the middle part, was chosen because it is

Table 1
Correspondence, for frequently occurring soil hues, between alphanumeric Munsell notation and angular notation $H°$

H_{Munsell}	$H°$
7.5 R	27
10 R	36
2.5 YR	45
5 YR	54
7.5 YR	63
10 YR	72
2.5 Y	81
5 Y	90
5 GY	126
5 G	162
5 B	234

Table 2
Quantification of uncemented phases

Field quantification scale (%)	Optimised central proportions (%)
0	0
[0–1]	1
[1–5]	5
[5–15]	15
[15–30]	30
[30–50]	45
[50–75]	75
[75–95]	84.3
[95–100]	97.5
100	100

compatible with the quantification capabilities of an observer in the field. It is based on Munsell's chart for estimating the proportions of colour mottles and the system developed by Chatelin (1976) and Beaudou (1977) for quantification in the field of soil features.

The quantifications by interval made with the aid of this scale were converted into central proportions by optimisation, under the constraint of the boundaries of each interval. This optimisation enabled us to centre the sum of the proportions obtained for each SV around 100% (Blavet, 1996). These optimised central proportions (cf. Table 2) were finally weighted for each SV, so that the sum of the weighted proportions of the uncemented phases of each SV were exactly equal to 100%.

Ten variables were obtained from the three numerical colour components and the weighted proportions of the different uncemented phases:

- Four variables were obtained from the colour of the principal uncemented phase of each SV. This is the phase whose weighted proportion is highest, or, when there is no such predominant phase, the matrix of the material. These four variables are the Munsell value, chroma and angular hue of colour (V_{phase1}, C_{phase1} and $H^{\circ}_{\text{phase1}}$, and its redness rating ($\text{RR}_{\text{phase1}}$).
- Four "mean colour" variables were calculated as functions of the colours and weighted proportions of the various uncemented phases of each SV. These variables are:

$$\cdot \text{ mean Munsell value, } \overline{V} = \Sigma(\alpha i \times Vi) \tag{6}$$

$$\cdot \text{ mean chroma, } \overline{C} = \Sigma(\alpha i \times Ci) \tag{7}$$

$$\cdot \text{ mean angular hue, } \overline{H^{\circ}} = \Sigma(\alpha i \times H^{\circ} i) \tag{8}$$

$$\cdot \text{ mean redness rating, } \overline{\text{RR}} = \Sigma(\alpha i \times \text{RR}i) \tag{9}$$

where Vi, Ci, $H^{\circ}i$, $\text{RR}i$ are, respectively, the Munsell values, chromas, angular hues and redness ratings of the different uncemented phases within the same soil volume, and αi is the weighted proportion of the different uncemented phases of this volume ($\Sigma \alpha i = 100\%$).

- Two further variables were obtained by calculating the barycentric colour, which is, for each SV, the barycentre of the colours of all the uncemented phases. This calculation was made in order to estimate the colour resulting from mixing the different phases of each SV; it is based on tests run on a computer screen using a Munsell-RVB converter (GretagMacbeth, 1998), which showed that this barycentre is close to the colour perceived when the phases are organised in juxtaposed micro-phases.

To calculate this barycentre, the cylindrical coordinates *Vi*, *Ci* and *H°i* of the Munsell colour of each uncemented phase were first converted into Cartesian coordinates *Xi*, *Yi* and *Zi*, using Eqs. (10)–(12).

$$\cdot\ Xi = Vi \tag{10}$$

$$\cdot\ Yi = Ci\cos\left(\frac{\pi H°i}{180}\right) \tag{11}$$

$$\cdot\ Zi = Ci\sin\left(\frac{\pi H°i}{180}\right) \tag{12}$$

The Cartesian coordinates of this barycentre (X_{bary}, Y_{bary}, Z_{bary}) were then calculated as a function of the weighted proportions αi of the different phases, using Eqs. (13)–(15).

$$\cdot\ X_{bary} = \Sigma(\alpha i \times Xi) = \Sigma(\alpha i \times Vi) = \overline{V}, \text{from Eqs. (6) and (10).} \tag{13}$$

$$\cdot\ Y_{bary} = \Sigma(\alpha i \times Yi) \tag{14}$$

$$\cdot\ Z_{bary} = \Sigma(\alpha i \times Zi) \tag{15}$$

Lastly, the barycentric colour variables ($\overline{V}_{bary}$, $\overline{C}_{bary}$ and $\overline{H°}_{bary}$) were obtained by converting the Cartesian coordinates of the barycentre into cylindrical coordinates in the Munsell colour cylinder, using Eqs. (16)–(18):

$$\cdot\ \text{barycentric value, } \overline{V}_{bary} = X_{bary} = \overline{V} \text{ from Eq. (13)} \tag{16}$$

$$\cdot\ \text{barycentric chroma, } \overline{C}_{bary} = \sqrt{(Y_{bary})^2 + (Z_{bary})^2} \tag{17}$$

$$\cdot\ \text{barycentric angular hue, } \overline{H°}_{bary} = \begin{cases} 360 + \left(\frac{180}{\pi}\Theta\right) si\Theta < 0 \\ \frac{180}{\pi}\Theta si\Theta \geq 0 \end{cases}$$

$$\text{with } \Theta = A\tan 2\left(\frac{Y_{bary}}{\sqrt{(Y_{bary})^2 + (Z_{bary})^2}}, \frac{Z_{bary}}{\sqrt{(Y_{bary})^2 + (Z_{bary})^2}}\right) \tag{18}$$

Since barycentric value ($\overline{V}_{bary}$) is equal to mean Munsell value ($\overline{V}$), this calculation provided two new variables, barycentric chroma ($\overline{C}_{bary}$) and barycentric angular hue ($\overline{H^{\circ}}_{bary}$). These two variables depend on both chromas and angular hues of the uncemented phases, based on Eqs. (11) and (12). In geometrical terms, however, $\overline{C}_{bary}$ is nothing other than the distance between the axis of the Munsell colour cylinder and the geometrical point of the barycentre of the colours. This distance is independent of the hue segment in which the barycentre is located, so it does not depend on the absolute positions of the hues of the uncemented phases on the circle of hues, only on their relative positions, i.e., the angular difference of hues.

3.3. Plotting sequences of $\overline{WLG}$ and soil colour variables

Geostatistical interpolations (Matheron, 1971) were carried out with Geo-Eas software (EPA, 1988) between points of $\overline{WLG}$ as well as points of values of the soil colour variables. For each of these variables, two directional variograms were computed, following vertical and slope directions. The variograms parameters (mathematical model, nugget, sill and ranges) were used for anisotropic kriging, giving regular data grids as results. Finally, these grids were converted in Surfer grid files (Keckler, 1994) to plot sequences with this software.

3.4. Relating the variables derived from soil colour to the mean annual soil waterlogging rate

The elementary soil volume corresponding to each vertical point used for calculating mean annual soil waterlogging rate was determined for each hydropedological station. This was done by taking the elevation of each point and the vertical boundaries of each SV, based on the piezometric and pedological databases. For the entire toposequence, this established 574 pairs associating an SV with a $\overline{WLG}$ value. Taking the 10 colour variables for each SV (V_{phase1}, $\overline{V}$ ($=\overline{V}_{bary}$), C_{phase1}, $\overline{C}$, $\overline{C}_{bary}$, H°_{phase1}, $\overline{H^{\circ}}_{bary}$, RR_{phase1} and $\overline{RR}$), 10 sets of 574 pairs of values associating a colour variable value with a mean annual soil waterlogging rate ($\overline{WLG}$) were thus obtained.

From these 10 sets of pairs of values, the following statistical analysis were carried out.

Table 3
Characteristics of annual and mean annual soil waterlogging rates ($n=630$)

Variable	Min	Max	Mean	Standard deviation
$WLG_{[89-90]}$	0	100	26.9	36.5
$WLG_{[90-91]}$	0	100	27.9	37.7
$WLG_{[91-92]}$	0	100	26.7	35.0
$\overline{WLG}$	0	100	27.7	35.4

Table 4
Inter-annual correlations between annual soil waterlogging rates

$WLG_{[year1]}/WLG_{[year2]}$	No. of pairs	Slope	r^2
$WLG_{[89-90]}/WLG_{[90-91]}$	630	1.02	0.95
$WLG_{[89-90]}/WLG_{[91-92]}$	630	0.95	0.94
$WLG_{[90-91]}/WLG_{[91-92]}$	630	0.92	0.93

(a) Each set was first analysed in search of a possible regression model f (linear or non-linear), such that $f(x) = \overline{WLG}$, where x is a colour variable (although colour variables can be considered as dependant variables in a deterministic point of view, $\overline{WLG}$ is here considered as the dependant variable both in a statistical and an operational point of view).

(b) For each model identified, the significance of the correlation coefficient obtained was analysed, by comparing this coefficient with the critical thresholds $r_{c0.95}$ and $r_{c0.99}$.

(c) For models associated with a significant correlation coefficient, the 95% confidence error margins and intervals of prediction of $\overline{WLG}$ were estimated. Taking account of the nature of the models, i.e., non-linear models with margins of error that varied according to colour variable, it has been assumed for each observed colour variable value x_h, that the real values $\overline{WLG}_h$ of the mean annual soil waterlogging rates would follow a normal distribution, with a mean of $f(x)$ and a standard deviation $\sigma\overline{WLG}_h$ given as:

$$\sigma\overline{WLG}_h = \sqrt{\sum_{i=1}^{i=n} \frac{(y_{ih} - f(x))^2}{n-1}} \tag{19}$$

Having calculated $\sigma\overline{WLG}_h$, from the model's data, a standard deviation function $g(x)$ for all possible values of x was determined by regression, such that $\sigma\overline{WLG} = g(x)$.

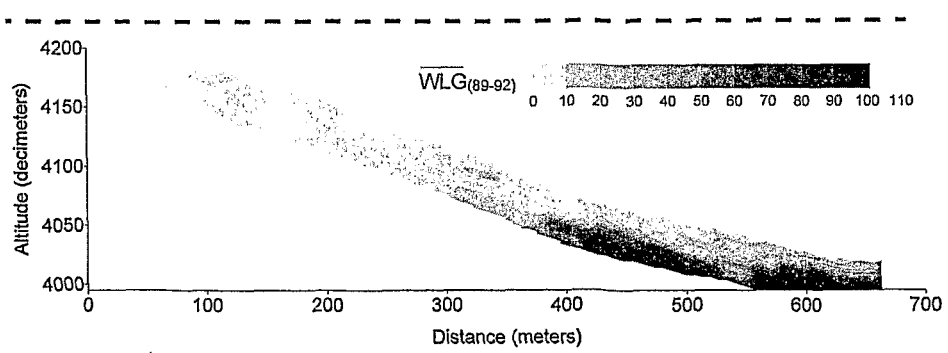

Fig. 3. Sequence of mean annual soil waterlogging rate.

Table 5
Colour characteristics of SVs

Variable	No. of SVs	Min	Max	Mean	Standard deviation	CV (%)
$H°_{phase1}$	144	36	234	69.4	24.3	35
$\overline{H°}$	144	36	217	68.0	20.1	30
$\overline{H°}_{bary}$	144	36	164	60.5	17.5	29
V_{phase1}	144	3	8	5.7	1.3	23
$\overline{V}$, $\overline{V}_{bary}$	144	3	8	5.6	1.0	18
C_{phase1}	144	1	8	3.8	2.3	60
$\overline{C}$	144	1	8	4.2	1.6	38
$\overline{C}_{bary}$	144	0.3	8	4.8	1.5	31
RR_{phase1}	144	−7.5	20	2.4	6.0	250
$\overline{RR}$	144	−6.7	16.5	2.7	4.8	178

This $g(x)$ function allowed to calculate the 95% confidence error margin of prediction of $\overline{WLG}$ for all possible values of x which, according to the probabilities of the laws of normal distribution, is given as:

$$E\overline{WLG}_{0.95}[x] = 1.96\,g(x). \tag{20}$$

Then, the 95% confidence interval of prediction of $\overline{WLG}$ for all possible values of $x(I\overline{WLG}_{0.95}[x])$ was calculated, as follows:

$$I\overline{WLG}_{0.95}[x] = \min\left(100, f(x) + E\overline{WLG}_{0.95}[x]\right) - \max\left(0, f(x) - E\overline{WLG}_{0.95}[x]\right). \tag{21}$$

(d) A provisional comparison of how well the different models fitted the data was made by a statistical examination of the differences between correlation coefficients. This examination led to the calculation of the correlation difference probability $P(\rho 1 \neq$

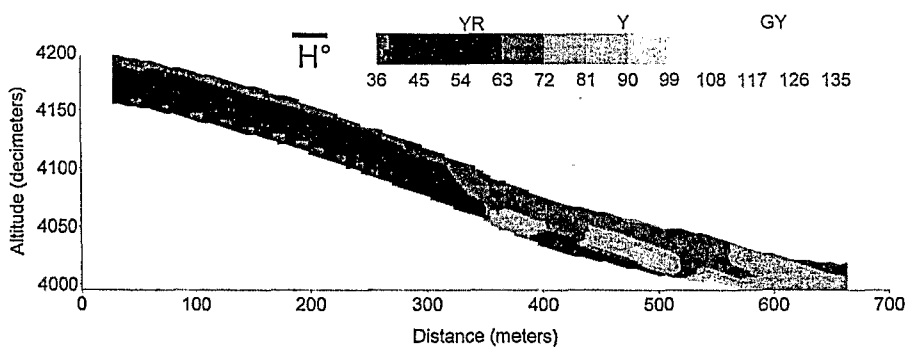

Fig. 4. Sequence of mean angular hue.

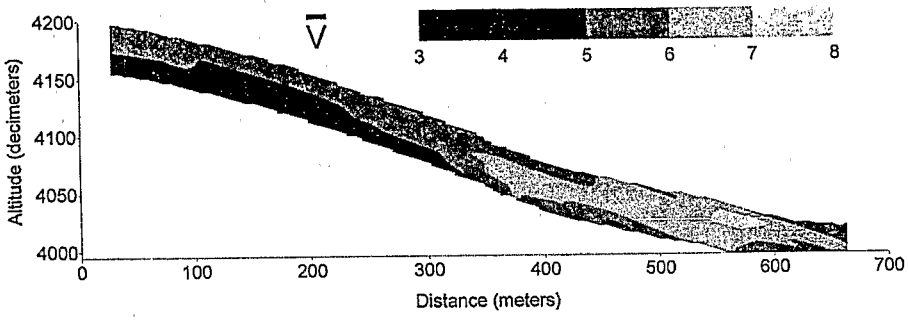

Fig. 5. Sequence of mean Mussell value.

$\rho 2$), which is a function of the value of these coefficients and the number of pairs of values. According to Baillargeon (1989), this probability is equal to:

$$\int_{-z}^{+z} \frac{1}{\sqrt{2\pi}} e^{\frac{-x2}{2}} dx, \text{ with } Z = \frac{z'_1 - z'_2}{\sqrt{\frac{1}{n_1 - 3} + \frac{1}{n_2 - 3}}} \tag{22}$$

where n_1, n_2 are the numbers of pairs of values for r_1, r_2, respectively and where z'_1 and z'_2 are the Fisher transforms of r_1 and r_2, such that:

$$z' = \frac{1}{2} \ln\left(\frac{1+r}{1-r}\right). \tag{23}$$

(e) For the models that best fit the data, a second comparison was made by examining the variations of $E\overline{\text{WLG}}_{0.95}[x]$ and $I\overline{\text{WLG}}_{0.95}[x]$

4. Results

4.1. Annual and mean annual soil waterlogging rates

Table 3 shows the global statistical characteristics of the annual soil waterlogging rates ($\text{WLG}_{[89-90],\ [90-91],\ [91-92]}$) and mean annual soil waterlogging rate $\overline{\text{WLG}}_{[89-92]}$

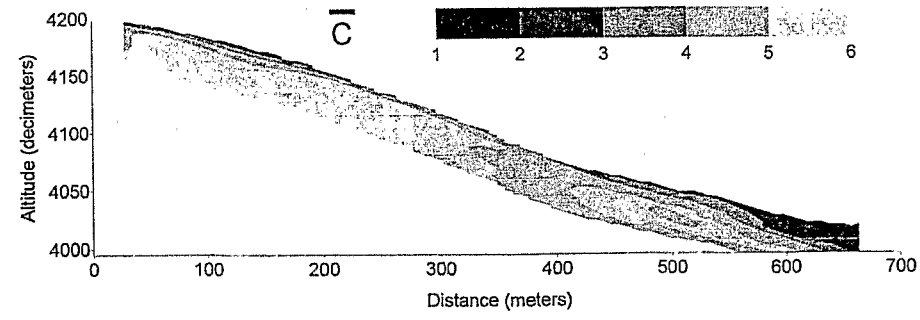

Fig. 6. Sequence of mean chroma.

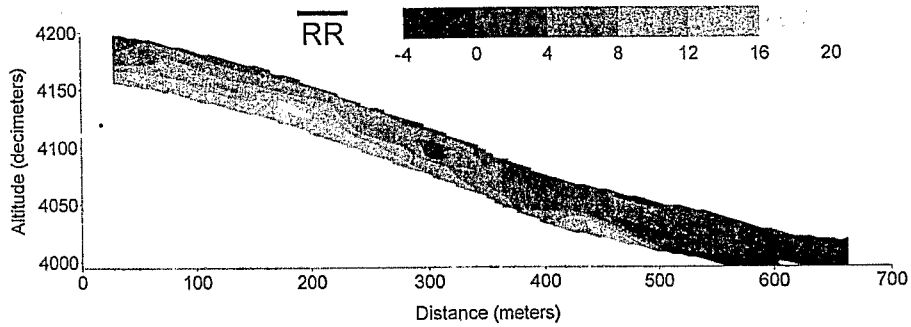

Fig. 7. Sequence of mean redness rating.

given as $\overline{WLG}$ for simplicity) obtained for the 630 points of the toposequence. It can be seen that these rates vary each year between 0 and 100 (cf. min and max values) and that the results obtained for any given year are close to those obtained for any other year (cf. mean and standard deviation). The narrowness of the inter-annual variations in WLG are confirmed by the strong linear correlation between these rates shown in Table 4, whichever 2 years are compared (adjustment on a slope close to 1 and $r^2 > 0.93$ for 630 pairs).

In view of these results and the fact that rainfall during the study period was representative of the mean rainfall conditions at the studied site, one can consider that the mean annual soil waterlogging rates obtained are similar to those that would be obtained for a longer period of readings.

Fig. 3 shows the spatial variations of $\overline{WLG}$ derived from anisotropic kriging of the 630 values obtained for the toposequence as a whole (Blavet, 1996). $\overline{WLG}$ is below 10 in the upper part of the toposequence, then increases rapidly at some depth in the middle part, reaching its highest values at the bottom, as expected.

4.2. Soil colour

Table 5 shows minimum, maximum, mean, standard deviation and variation coefficient for each of the colour variables of the 144 SVs of the toposequence. There are marked differences between the colour of the principal phase and those for mean colour and barycentric colour. In the first place, the mean values differ, although the orders of magnitude are the same, and secondly, the colour of the principal phase always varies

Table 6
Linear correlation coefficients r, and comparison with $r_{c0.95}$

x	y	No. of pairs	r	$r_{c0.95}$	Significance
C_{phase1}	$\overline{ENG}$	574	0.008	0.08	n.s.
$\overline{C}$	$\overline{ENG}$	574	−0.06	0.08	n.s.
$\overline{C}_{bary}$	$\overline{ENG}$	574	−0.07	0.08	n.s.

Table 7
Parameters of exponential models

x	$f(x)$	α	β	No. of pairs	r	$r_{c0.99}$	Significance
V_{phase1}	$\overline{ENG}$	0.02	1.07	574	0.25	0.107	$r>0^a$
$\overline{V}$	$\overline{ENG}$	0.07	0.87	574	0.35	0.107	$r>0^a$

[a]Significant to 99%.

more than the mean colour and barycentric colour (cf. extreme values, standard variations and variation coefficients).

Spatial variations in mean colour across the toposequence are shown in Figs. 4–7 which were obtained by anisotropic kriging of the mean colour variable values of the 144 SVs (Blavet, 1996). As with the $\overline{WLG}$ sequence in Fig. 3, these sequences also show sharp variations between the uphill and downhill parts of the toposequence. Thus from the middle of the toposequence, $\overline{H^\circ}$ becomes generally yellower than it is further uphill, reaching values of over 63. Similarly, $\overline{V}$ increases to over 6 further downhill, while for $\overline{C}$, values of less than 4 become widespread. Mean redness rating ($\overline{RR}$) diminishes from top to bottom of the slope, falling below 4 near the bottom.

4.3. Relationships between soil colour and $\overline{WLG}$

From an analysis of data sets associating each colour variable with $\overline{WLG}$, three different cases emerge.

- No connection can be seen between chroma variables and $\overline{WLG}$. The dispersion diagrams combining these variables show random patterns. This randomness particularly reflects the fact that the linear correlation coefficients r are not significantly different from 0 (cf. Table 6), since they are in all cases below the critical threshold $r_{c0.95}$.
- The relations between the Munsell value variables and $\overline{WLG}$ are non-linear, corresponding to exponential regression models in the following form:

$$\overline{WLG}=f(x)=\alpha e^{\beta x} \tag{24}$$

where x is the Munsell value variable, and α and β are constants. Non-linear regression analysis gives the values of α and β shown in Table 7. These relationships

Table 8
Parameters of logistic models

x	$f(x)$	a	b	No. of pairs	r	$r_{c0.99}$	Significance
H°_{phase1}	$\overline{ENG}$	18551	−0.11	574	0.57	0.107	$r>0^a$
$\overline{H^\circ}$	$\overline{ENG}$	382353	−0.16	574	0.72	0.107	$r>0^a$
$\overline{H^\circ}_{bary}$	$\overline{ENG}$	200038	−0.16	574	0.68	0.107	$r>0^a$
RR_{phase1}	$\overline{ENG}$	2.67	1	574	0.52	0.107	$r>0^a$
$\overline{RR}$	$\overline{ENG}$	2.07	1	574	0.72	0.107	$r>0^a$

[a]Significant to 99%.

Table 9
Constants $c1$, $c2$, $c3$ and $c4$ of the 95% confidence error margins of predictions of the mean annual soil waterlogging rate ($E\overline{WLG}_{0.95}[x]$)

x	$c1$	$c2$	$c3$	$c4$
$H°_{phase1}$	2199	21.4	94.1	3
$\overline{H°}$	808	9.8	77.9	3
$H°_{bary}$	836	8.9	76.5	3
RR_{phase1}	400	3	−2.5	3
$\overline{RR}$	200	2.8	−0.5	2

are significant, since the correlation coefficients r are above the critical threshold $r_{c0.99}$ (cf. Table 7). But the relatively small values of these coefficients show that there is still a wide variation in $\overline{WLG}$ which is not explained by the models.

- The dispersion diagrams obtained by comparing the angular hue and redness rating variables with the $\overline{WLG}$ variable show sigmoidal relationships. These relationships correspond to logistic regression models (Jolivet, 1983; Tomassone et al., 1992), of the general form:

$$\overline{WLG} = \frac{100}{1 + (ae^{bx})} \tag{25}$$

where x is the angular hue or redness rating variable and a and b the constants of the model. Non-linear regression analysis gives the values of constants a and b, as shown in Table 8.

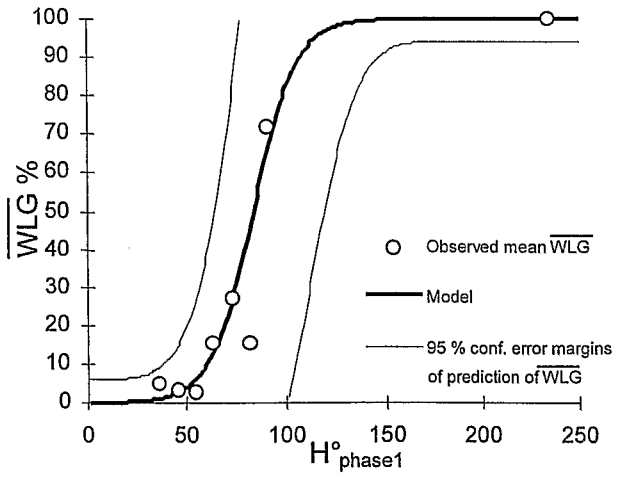

Fig. 8. $\overline{WLG} = f(H°_{phase1})$ relationship and 95% confidence error margins of prediction.

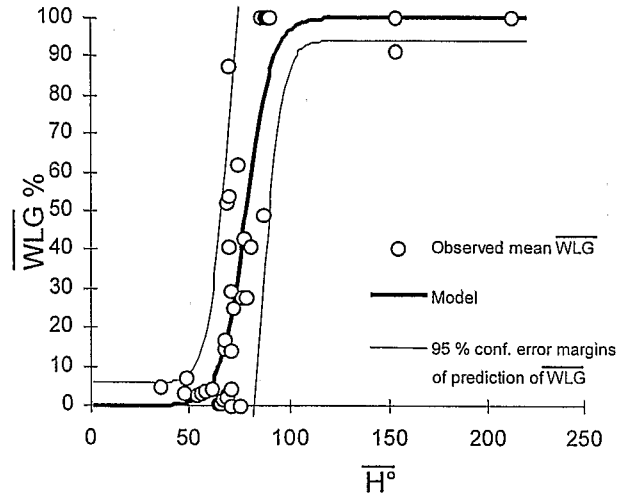

Fig. 9. $\overline{\mathrm{WLG}} = f(H°)$ relationship and 95% confidence error margins of prediction.

In all cases, these logistical models fit the data well. The r correlation coefficients (cf. Table 8), are significantly higher than the critical thresholds $r_{c0.99}$, which allows to assert with 99% confidence that there is a logistic relationship between the angular hue and redness rating variables and $\overline{\mathrm{WLG}}$.

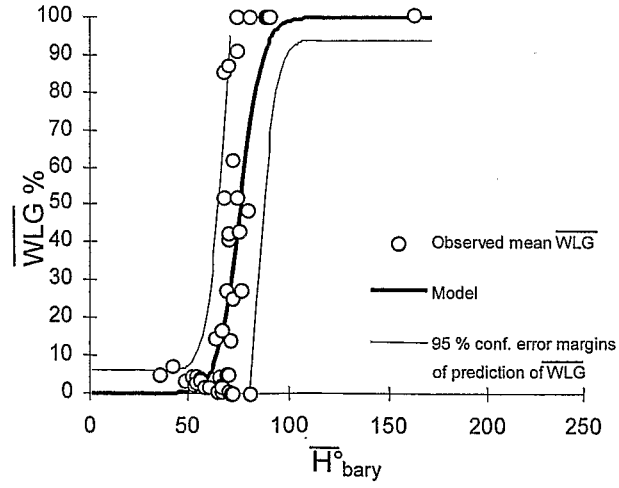

Fig. 10. $\overline{\mathrm{WLG}} = f(H°_{\mathrm{bary}})$ relationship and 95% confidence error margins of prediction.

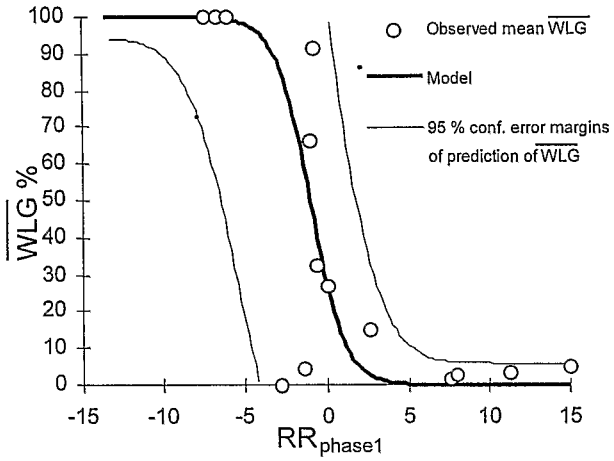

Fig. 11. $\overline{\mathrm{WLG}} = f(\mathrm{RR}_{\mathrm{phase1}})$ relationship and 95% confidence error margins of prediction.

For all these logistic models, the 95% confidence error margin of prediction of $\overline{\mathrm{WLG}}$ ($E\overline{\mathrm{WLG}}_{0.95}[x]$) obeys a Gaussian law in the following general form:

$$E\overline{\mathrm{WLG}}_{0.95}[x] = 1.96\,g(x) = 1.96\left[\frac{c1}{c2\sqrt{2\pi}}\mathrm{e}^{-0.5\left(\frac{x-c3}{c2}\right)^2} + c4\right] \tag{26}$$

where $g(x)$ is a function, determined by regression analysis, which gives the standard deviation of $\overline{\mathrm{WLG}}$ (cf. Methods) and $c1$, $c2$, $c3$ and $c4$ are the constants shown in Table 9.

From these results Figs. 8–12 were obtained, which show the curves of the various logistic models $\overline{\mathrm{WLG}} = f(x)$ and their associated 95% confidence error margins of prediction $\overline{\mathrm{WLG}} \pm E\overline{\mathrm{WLG}}_{0.95}[x]$.

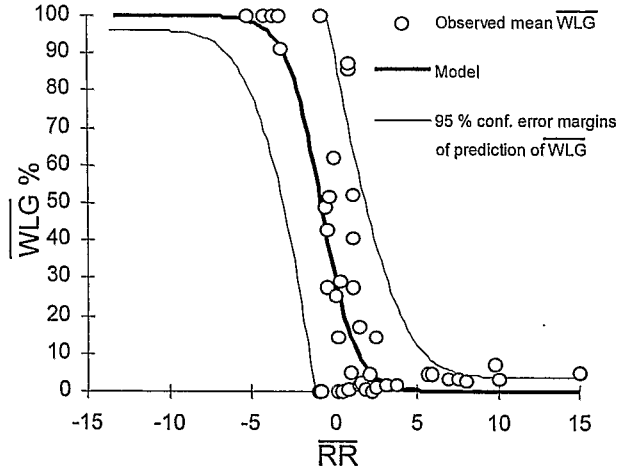

Fig. 12. $\overline{\mathrm{WLG}} = f(\overline{\mathrm{RR}})$ relationship and 95% confidence error margins of prediction.

5. Discussion

5.1. Comparison and classification of the regression models

Apart from the chroma variables, which seem to be unrelated to $\overline{WLG}$, all the other colour variables (Munsell value, angular hue and redness rating variables) are linked to the $\overline{WLG}$ variable by non-linear regression models, with correlation coefficients significant to 99%. A priori, all these variables therefore seem to be usable for predicting $\overline{WLG}$, more or less accurately. In practice, a comparison of the different models shows that some of these variables are more suitable for making this prediction than others.

Firstly, some colour variables are more closely related to $\overline{WLG}$ than others. The correlation difference probabilities $P(\rho 1 \neq \rho 2)$, which are a function of the value of the correlation coefficients and the number of pairs of values (see Methods) classifies the Munsell value, angular hue and redness rating variables into three groups.

(1) Angular hue and redness rating variables depending on the various uncemented phases ($\overline{H^\circ}$, $\overline{H^\circ_{bary}}$ and $\overline{RR}$), are most closely linked to $\overline{WLG}$. The logistic models established from these variables have comparable correlation coefficients ($P(\rho 1 \neq \rho 2) < 95\%$) of around 0.7 (cf. Table 10), which are significantly higher than those of the other models ($P(\rho 1 \neq \rho 2) > 99\%$).

(2) The angular hue and redness rating variables of the main uncemented phase (H°_{phase1} and RR_{phase1}) are less closely linked to $\overline{WLG}$. The logistic models established from these variables have statistically comparable correlation coefficients ($P(\rho 1 \neq \rho 2) < 95\%$) of about 0.55.

(3) The Munsell value variables (V_{phase1} and $\overline{V}$) are least closely linked to $\overline{WLG}$ with comparable correlation coefficients ($P(\rho 1 \neq \rho 2) < 95\%$) of around 0.3.

This comparison favours the three logistic models based on $\overline{H^\circ}$, $\overline{H^\circ}_{bary}$ and $\overline{RR}$. However, these three models are not equivalent, given their associated 95% confidence error margins of prediction of the mean annual soil waterlogging rate ($E\overline{WLG}_{0.95}$). For if one compares these error margins (cf. Fig. 13), one can see first of all that the error margin is systematically narrower for the model based on $\overline{H^\circ}$ than for that based on $\overline{H^\circ}_{bary}$. On this basis it would seem preferable to exclude this latter model, especially as the calculation of barycentric angular hue is significantly more complex than that of

Table 10
Statistical comparison $P(\rho_1 \neq \rho_2)$, in %, between correlation coefficients obtained from different regression models

$r\overline{H^\circ}$ (= 0.72)	100					
$r\overline{H^\circ}_{bary}$ (= 0.68)	99.8	81.6[a]				
rRR_{phase1} (= 0.52)	77.1[a]	100	100			
$r\overline{RR}$ (= 0.72)	100	0[a]	81.6[a]	100		
rV_{phase1} (= 0.25)	100	100	100	100	100	
$r\overline{V}$ (= 0.35)	100	100	100	99.9	100	94[a]
	rH°_{phase1} (= 0.57)	$r\overline{H^\circ}$ (= 0.72)	$r\overline{H^\circ}_{bary}$ (= 0.68)	rRR_{phase1} (0.52)	$r\overline{RR}$ (= 0.72)	rV_{phase1} (= 0.25)

[a]correspond to non-significant differences (< 95%).

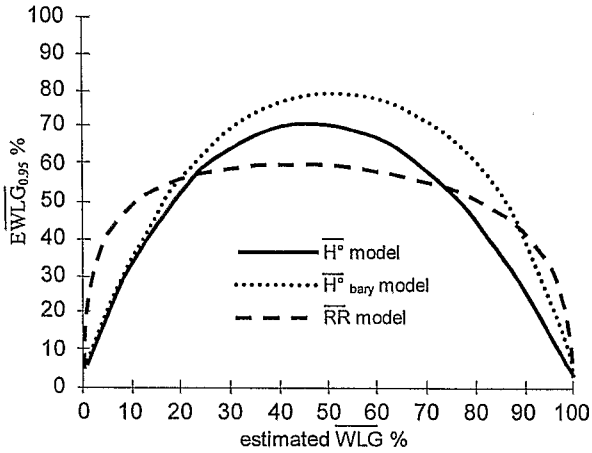

Fig. 13. 95% confidence error margins of prediction of the mean annual soil waterlogging rate ($\overline{EWLG}_{0.95}$), in relation to mean angular hue, barycentric angular hue and mean redness rating.

mean angular hue (cf. Methods). On the other hand, if one compares the error margins associated with the models based on $\overline{H°}$ and $\overline{RR}$, one finds that they do not justify systematically favouring either one of the two models. For although the error margin associated with the model based on $\overline{H°}$ is narrower than that associated with the model based on $\overline{RR}$ where the mean annual soil waterlogging rates estimated by the models are below 20% or above 90%, it is slightly wider for mean annual soil waterlogging rates within the 20–90% range.

It would therefore seem that the two models best suited to predicting mean annual soil waterlogging rate are the logistic models based on mean angular hue $\overline{WLG} = f(\overline{H°})$ and mean redness rating $\overline{WLG} = f(\overline{RR})$.

5.2. Comments on the classification obtained

The lack of any link between chroma variables and $\overline{WLG}$ can be directly explained by the meaning of these variables. Chroma is not connected with the nature of the colour, but with the degree of saturation of whatever colours are present (C_{phase1} and $\overline{C}$) or the degree of saturation of these colours and their angular difference in hue ($\overline{C}_{bary}$). As a result, soil materials of the same chroma may differ in colours, i.e., may have different spectral reflectances due to a range of mineralogical compositions and hydrological conditions.

The fairly weak link between the Munsell value variables and $\overline{WLG}$ may reflect a combination of relationships. It may be that although there is a tendency for the materials to become pale as groundwater leaches out minerals (Fritsch, 1993; Blavet, 1996), this tendency is partly masked by the effects of organic matter on Munsell value (Schulze et al., 1993).

The connection between angular hue and redness rating variables and $\overline{WLG}$ could be due to a link between these colour factors and the particular mineralogical form of iron

Table 11
Type of mottling SVs

No. of uncemented phases	No. of SVs	% of SVs
1	39	27
2	50	35
3	55	38

oxide present in the soil (Torrent et al., 1980, 1983; Fritsch et al., 1990b, Jeanroy et al., 1991; Schwertmann, 1993), which in turn usually depends on hydration or oxidation–reduction conditions in the materials in question (Segalen, 1969; Chauvel and Pedro, 1978).

Finally, it is not surprising that mean angular hue and mean redness rating should be more closely linked to $\overline{WLG}$ than the angular hue and redness rating of the main phase. For in the case in hand, the latter two variables only partly reflect the colour of the materials, since two-thirds of the 144 SVs contain more than one phase (cf. Table 11) and there can be quite major colour differences between these phases (up to five units of Munsell value, seven of chroma and 171° of angular hue).

5.3. Limitations on the use of logistic models based on mean angular hue and mean redness rating, and analysis of the dispersion of results

The value of the correlation coefficients r associated with the logistic models based on variables $\overline{H^\circ}$ and $\overline{RR}$ is 0.72. This value, significant to over 99% ($r_{c0.99} = 0.107$ for 574 pairs of values), is quite high compared to the values obtained for the other models. It nonetheless reflects a certain dispersion of results around the models, since 48% ($1 - r^2 = 0.48$) of total variations in mean annual soil waterlogging rate are not explained.

This dispersion is mainly concentrated in the upcurve of the curve, as is shown by the width of $I\overline{WLG}_{0.95}$ (i.e., the width of the 95% confidence interval of prediction of $\overline{WLG}$) in this domain (cf. Fig. 14). In this part of the curves, there is even a maximal zone of uncertainty for mean annual soil waterlogging rate (width of 95% confidence interval = 100 for mean angular hues of around 75°, i.e., 10 YR to 2.5 Y, or redness ratings close to 0), within which it is unrealistic to try to predict the mean annual soil waterlogging rate.

A priori, this dispersion is not due to the models chosen to describe the relationships, because it is spread across both sides of the curves of these models. It may be due to several natural causes: (1) materials with a Munsell hue of 10 YR to 2.5 Y and a redness rating close to 0 may be only weakly sensitive to variations in mean annual soil waterlogging rate; (2) the colours of some soil volumes (volumes with Munsell hue 10 YR–2.5 Y and redness rating close to 0) may not be linked to present-day hydrological conditions (this would apply, for example, to "fossil" soil volumes formed under hydrological conditions that no longer exist).

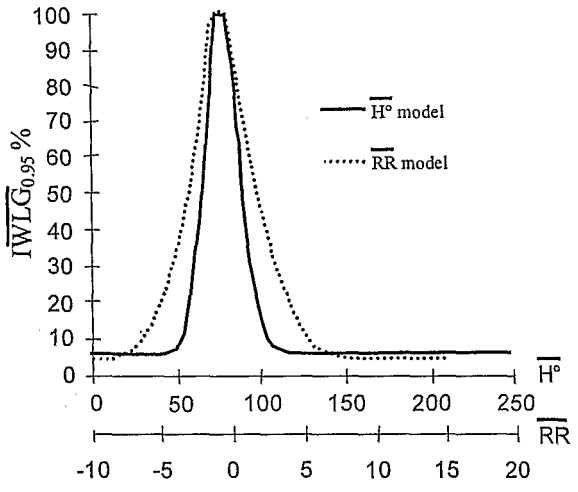

Fig. 14. 95% confidence interval of prediction of the mean annual soil waterlogging rate ($\overline{IWLG}_{0.95}$), in relation to mean angular hue and mean redness rating.

Some of the dispersion may be due to imprecision or bias introduced by the methods used to estimate colour:

- colour measurement on dry samples can introduce a bias because the hues of some samples may change during drying as iron re-oxidises;
- colour assessment with Munsell colour plates, which give only a limited number of reference colours, must also result in imprecision;
- estimation of the relative volumes of different uncemented phases when calculating mean angular hue and mean redness rating can also result in imprecision.

These methods could be improved:

- by measuring colour on-site using a colorimeter capable of distinguishing slight colour differences (Trouvé, 1991), especially for Munsell hues between 10 YR and 2.5 Y;
- by quantifying more precisely the relative volumes of the uncemented phases (it remains to be seen what analysis technique will be best here).

6. Conclusion

The results of this survey show that the mean hue and mean redness rating of a soil are linked to its mean annual soil waterlogging rate ($\overline{WLG}$) by logistic functions. Despite the existence of a maximal zone of uncertainty for the prediction of intermediate $\overline{WLG}$, accurate predictions of low $\overline{WLG}$ can be done from mean hues redder than 10 YR or redness ratings higher than 5, and accurate predictions of high $\overline{WLG}$ can be done from mean hues yellower than 2.5 Y or mean redness ratings lower than -5.

As long as no recent change occurred in the groundwater dynamic (for example, a change due to drainage work), these two colour variables should be easily obtained potential indicators of high or low annual duration of soil waterlogging, in hillsides of West Africa characterised by a tropical climate, a sharply contrasted dry season, a bedrock of granite and gneiss, an annual rainfall between 800 and 1200 mm, a savanna vegetation, and a soil mantle organised in toposequences on a red ferralitic weathering.

Acknowledgements

This was conducted as part of a joint program between ORSTOM (Institut Français de Recherche Scientifique pour le Développement en Coopération) and the Institut National des Sols, Togo. It was financed by the ORSTOM research unit on "soil behaviour, water uptake and yield build-up" (Département MAA). The experimental site was provided by Cirad (the French-based Centre International de Recherche Agronomique pour le Développement). Our special thanks to A. Forget and R. Mawussi for their valuable help in the field.

References

Baillargeon, G., 1989. Probabilités statistique et techniques de régression. In: Trois-Riviéres. Editions S.M.G. pp. 401–428.

Beaudou, A.G., 1977. Note sur la quantification et le langage typologique. Cah. ORSTOM, Ser. Pedol. XV (1), 35–41.

Beven, K., Kirkby, M.J., 1979. A physically based, variable contributing area model of basin hydrology. Hydrol. Sci. Bull. 24 (1–3), 43–69.

Blavet, D. 1994. Présentation sommaire de l'application Thorpedo (Traitement d'horizons par pédocomparateur). Application sous Paradox 3.5 pour Ms. Dos. ORSTOM, Montpellier, 19 pp.

Blavet, D. 1996. Hydropédologie d'un bassin versant représentatif d'un paysage sur socle granito-gneissique d'Afrique de l'ouest (Togo). Relations avec le comportement d'une plante cultivée. Thése de doctorat, Univ. Montpellier II, 236 pp.

Boulet, R. 1974. Toposéquences de sols tropicaux en Haute-Volta. Equilibres dynamiques et bioclimatiques. Thése Univ. Strasbourg, 330 pp.

Brand, E.W., Premchitt, J., 1980. Shape factors of cylindrical piezometers. Géotechnique 30 (4), 369–384.

Chatelin, Y. 1976. Une épistémologie des sciences du sol. Thése Univ. Dijon, 151 pp.

Chauvel, A., 1977. Recherches sur la transformation des sols ferrallitiques dans la zone tropicale è saisons contrastées, Coll. Travaux et documents ORSTOM Vol. 62, Paris, 532 pp.

Chauvel, A., Pedro, G., 1978. Genèse des sols beiges (ferrugineux tropicaux lessivés) par transformation des sols rouges (ferrallitiques) de Casamance (Sénégal). Cah. ORSTOM, Ser. Pedol. XVI (3), 231–249, (in French).

Chevallier, P. 1988. Complexité hydrologique du petit bassin versant. Exemple en savane humide: Booro-Borotou (Côte d'Ivoire). Thése Univ. Montpellier, 342 pp.

Depraetere, C., 1992. Demiurge 2.0. Chaîne de production et de traitement de modèles numériques de terrain, Coll. Logorstom. Paris, 198 pp.

Engman, E.T., Gurney, R.J., 1991. Remote Sensing in Hydrology. Remote Sensing Applications. Chapman & Hall, London, 225 pp.

EPA, 1988. Geo-Eas (Geostatistical Environmental Assessment Software). User's Guide. US Environmental Protection Agency, Las Vegas, 215 pp.

Evans. C.V., Franzmeier, D.P., 1986. Saturation, aeration and color patterns in a toposequence of soils in north-central Indiana. Soil Sci. Soc Am. J. 50, 975–980.
Evans. C.V., Franzmeier, D.P., 1988. Color index values to represent wetness and aeration in some Indiana soils. Geoderma 41, 353–368.
Faure. P., 1975. Les associations de sols rouges et jaunes au nord-ouest Dahomey. Caractéres des sols et des séquences. Cah. ORSTOM, Ser. Pedol. XIII (2), 119–157.
Franzmeier, D.P., Yahner, J.E., Steinhardt, G.C., Sinclair, H.R., 1983. Color patterns and water table levels in some Indiana soils. Soil Sci. Soc. Am. J. 57, 1196–1202.
Fritsch. E. 1993. Organisation et fonctionnement de "systèmes sols" en zone de contact forêtsavane du milieu tropical ouest africain. (Booro Borotou, Côte d'Ivoire). Coll. Etudes et thèses ORSTOM, Paris, 176 pp.
Fritsch. E.,Chevallier, P., Janeau, J.L. 1990a. Le fonctionnement hydrodynamique du bas de versant. Structure et fonctionnement hydropédologique d'un petit bassin versant de savane humide. Coll. Etudes et théses ORSTOM, Paris, pp. 185–206.
Fritsch. E., Valentin, C., Morel, P., Leblond, P. 1990. La couverture pédologique: interaction avec les roches, le modelé et les formes de dégradation superficielles. Structure et fonctionnement hydropédologique d'un petit bassin versant de savane humide. Coll. Etudes et théses ORSTOM, Paris, pp. 37–57.
Gavaud. M., 1970. Les grandes divisions du quaternaire de régions ouest-africaines établies sur des bases pédologiques, ORSTOM. Yaoundé, 21 pp.
Grandin, G., 1976. Aplanissements cuirassés et enrichissements des gisements de manganèse dans quelques régions d'Afrique de l'ouest. Coll. Mémoires ORSTOM 82, 276.
GretagMacbeth, 1998. Munsell Conversion Program. Disponible à www.munsell.com/cmc/index.htm.
Jeanroy, E., Rajot, J.L., Pillon, P., Herbillon, A.J., 1991. Differential dissolution of hematite and goethite in dithionite and its implication on soil yellowing. Geoderma 50, 81–94.
Jolivet, E., 1993. Introduction aux modèles mathématiques en biologie, Coll. Actualités scientifiques et agronomiques INRA 11, Masson, Paris, 151 pp.
Keckler, D, 1994. Surfer for Windows, Golden Software, User's Guide, Contouring and 3D Surface Mapping, Golden, CO. 230 pp.
Lelong. F., 1966. Régime des nappes phréatiques contenues dans les formations d'altération tropicale. Conséquences pour la pédogenèse. Sciences de la Terre (2). In: Fond. Scient. Géol. App., Nancy. pp. 201–244.
Lenoir, F., 1977. Le régime des nappes dans les formations d'altération. In: Un exemple en Côte d'Ivoire (Sakassou-Toumodi). ORSTOM, Abidjan,. p. 48.
Leprun. J.C. 1979. Les cuirasses ferrugineuses des pays cristallins de l'Afrique occidentale sèche. Genèse Transformations -Dégradation. Thèse Univ. Strasbourg and Sci. Géol. Strasbourg, 58, 253 pp.
Levêque, A. 1975. Pédogenèse sur le socle granito-gneissique du Togo. Différenciation des sols et remaniements superficiels. Thèse Univ. Strasbourg, 301 pp.
Mathé, E., 1993. Etude de toposéquences et cartographie pédologique détaillée à 1/3.000ème. In: Exemple d'étude du site expérimental IRCT de Dalanda (Centre Togo). ORSTOM-INS, Lomé. p. 100.
Matheron, G., 1971. The theory of regionalised variables and their applications. In: Les Cahiers du Centre de Morphologie Mathématique, fasc. 5, Centre de géostatistique, Fontainebleau. p. 212.
Mokma, D.L., Cremeens, D.L., 1991. Relationships of saturation and B horizon colour patterns of soils in three hydrosequences in south-central Michigan, USA. Soil Use Manage 7, 56–61.
Mokma, D.L., Sprecher, S.W., 1994. Water table depths and color patterns in soils developed from red parent materials in Michigan, USA. Catena 22, 287–298.
Munsell, A.H. 1946, A color notation, Munsell Color, Baltimore MD.
Munsell Color, 1976. Munsell Book of Color. Matte Finish Collection, Baltimore, MD.
Poss, R., Roussel, B., Jallas, E., 1990. Relations entre les caractères du milieu et les espèces ligneuses au Nord-Togo. Rev. Ecol. (Terre Vie) 45, 7–24.
Poss, R., Valentin, C., 1983. Structure et fonctionnement d'un système eau–sol–végétation: une toposéquence ferralitique de savane (Katiola-Côte d'Ivoire). Cah. ORSTOM, Ser. Pedol. 20 (4), 341–360.
Schulze, D.G., Nagel, J.L., Van Scoyoc, G.E., Henderson, T.L., Baumgardner, M.F., 1993. Significance of organic matter in determining soil colors. In: Soil Color. Soil Sci. Soc. Am. Spec. Publ. No. 31, Madison pp. 71–90.

Schwertmann, U., 1993. Relations between iron oxides, soil color, and soil formation. In: Soil Color. Soil Sci. Soc. Am. Spec. Publ. No. 31, Madison pp. 51–69.

Segalen, P., 1969. Contribution à la connaissance de la couleur des sols à sesquioxydes de la zone intertropicale: sols jaunes et sols rouges. Cah. ORSTOM, Ser. Pedol. 7 (2), 225–236.

Smith, M.C., Vellidis, G., Thomas, D.L., Breve, M.A., 1992. Measurement of water table fluctuations in a sandy soil using ground penetrating radar. Trans. ASAE 35 (4), 1161–1166.

Thompson, J.A., Bell, J., 1996. Color index for identifying hydric conditions for seasonally saturated mollisols in Minnesota. Soil Sci. Soc. Am. J. 60, 1979–1988.

Tomassone, R., Audrain, S., Lesquoy-de Turckeim, E., Millier, C., 1992. La régression. Nouveaux regards sur une ancienne méthode statistique, Coll. Actualités scientifiques et agronomiques INRA, No. 13 . Masson, Paris, 188 pp.

Torrent, J., Schwertmann, U., Fechter, H., Alferez, F., 1983. Quantitative relationships between soil color and hematite content. Soil Sci. 136 (6), 354–358.

Torrent, J., Schwertmann, U., Schulze, D.G., 1980. Iron oxide mineralogy of some soils of two river terrace sequences in Spain. Geoderma 23, 191–208.

Trouvé, A., 1991. In: La mesure de la couleur. Principes, technique et produits du marché. Afnor-Cetim. p. 193.

USDA Soil Survey Staff, 1975. Mottles that have chroma of 2 or less. In: Soil Taxonomy: A Basic System of Soil Classification for Making and Interpreting Soil Surveys. Agriculture Handbook Vol. 436, pp. 48–49.

Vizier, J.F., 1974a. Recherche de relations morphogénétiques existant dans un type de séquence de sols hydromorphes peu humifères au Tchad. 1ère partie: Etude des caractères morphologiques et analytiques des sols de la séquence de Gole. Cah. ORSTOM, Ser. Pedol. 12 (2), 171–206, (in French).

Vizier, J.F., 1974b. Recherche de relations morphogénétiques existant dans un type de séquence de sols hydromorphes peu humifères au Tchad: 2ème partie: Dynamique de l'eau et du fer dans les sols de la séquence: 3ème partie: conclusions sur l'évolution actuelle des sols et hypothèse sur la formation de la séquence. Cah. ORSTOM, Ser. Pedol. 12 (3), 211–266.

Vizier, J.F., 1984. Les phénomènes d'hydromorphie en régions tropicales à saisons contrastées. Application à une meilleure caractérisation des concepts de gley et de pseudogley. Sci. Sol. Bull. AFES 3, 225–238.

Vizier, J.F., 1992. Eléments pour l'établissement d'un référentiel pour les solums hydromorphes. Référentiel pédologique. Principaux sols d'Europe. Coll. Techniques et pratiques, INRA, Paris, 193–207.

Worou, S., 1988. Les nappes perchées semi-permanents: bien les connaître pour mieux les utiliser. Comm. 97 Réu. Cor. Des sols. FAO Cotonou, 14–23 Nov., 1988. Rapp. FAO Vol. 63, 202–207.